Available online at www.sciencedirect.com
ScienceDirect
Optik 119 (2008) 419–423
Optik Optics
www.elsevier.de/ijleo

4-D imaging of fluid flow with digital in-line holographic microscopy

J. Garcia-Sucerquia*,[1], W. Xu, S.K. Jericho, M.H. Jericho, H.J. Kreuzer

Department of Physics and Atmospheric Science, Dalhousie University, Halifax, Nova Scotia, Canada B3 H 3J5

Received 17 October 2006; accepted 16 January 2007

Abstract

The large depth of field of digital in-line holographic microscopy (DIHM) with numerical reconstruction provides an ideal tool for the study of microfluidic phenomena. As indicators of the flow patterns we use latex microspheres and also red blood cells whose three-dimensional trajectories and velocities can easily be measured as a function of time with subsecond and micron resolution. We demonstrate the efficiency of DIHM by showing 3-D views of the flow patterns around big spheres in various geometric arrangements.

Keywords: Digital holography; Microfluidics; Three-dimensional rendering

1. Introduction

The efficient recording of the trajectories of particles that are moving throughout a 3-D space has been an important problem in several branches of science such as colloidal suspensions, the motion of algae or larvae in water, the motion of bacteria around and in cells, and the characterization of marine particulates [1–7]. Since microfluid flow is generally at low Reynolds numbers, vortex mixing in microchannels does not occur and it is important to capture experimentally the effectiveness of methods that may be devised to produce mixing.

Another important microfluidics area is the study of fluid flow induced by the locomotion of microorganisms such as algae and various plankton species. This is a particularly challenging field since it is difficult with standard microscopic methods to simultaneously follow the motion of the organism as well as that of tracer particles that may be in its vicinity but are sufficiently removed to be out of focus.

Modern micromachining methods have allowed the construction of microfluidic devices that have had a particularly significant impact on the development of novel biomedical instrumentation. Some of these involve the motion of macromolecules, vesicles or even whole cells through narrow channels and the flow can also be accompanied by biochemical processes between suspended components or with the channel walls. Other device applications involve the separation of cells in fluid channels with the help of electrophoretic or dielectrophoretic forces [1–3]. Other MEMS devices have been developed in order to facilitate the mixing of two fluids at the microfluid scale. Particle image velocimetry systems described in the literature [4–6] are generally based on conventional optical microscopy. To overcome the limited depth of field available in conventional optical microscopy holographic methods have been developed of which digital in-line holographic microscopy (DIHM) as developed in our group [7–11]

*Corresponding author.
E-mail address: jigarcia@fizz.phys.dal.ca (J. Garcia-Sucerquia).
[1]On leave from Physics School Universidad Nacional de Colombia Sede Medellín, A.A. 3840, Medellín, Colombia.

0030-4026/$ - see front matter © 2007 Published by Elsevier GmbH.
doi:10.1016/j.ijleo.2007.01.004

seems an ideal tool to capture the 3-D motion of micron-sized particulates in fluids with temporal and spatial resolution at the subsecond and micron level. The advantages of DIHM, apart from its high resolution, are (1) the simplicity of instrumentation, (2) the availability of a fast reconstruction algorithm, (3) a simple procedure to capture many particle trajectories throughout a sample volume.

2. Experimental method

The experimental setup of DIHM is illustrated in Fig. 1. The coherent light from a laser is focused onto a pinhole from which spherical waves emerge that illuminate a nearby object. On the detector chip of a CCD camera, placed a short distance from the object, waves that are scattered by the object combine with unscattered waves from the pinhole (the reference waves) to form an interference pattern or hologram.

To obtain high-resolution DIHM reconstruction images of the movement trajectories of the objects in a tank, we proposed the following procedure [7,11]: (i) a sequence of holograms (h_i) is recorded by a CCD camera with a sufficiently high capture rate and transferred to a computer; (ii) undesired background effects are eliminated by subtracting consecutive holo-

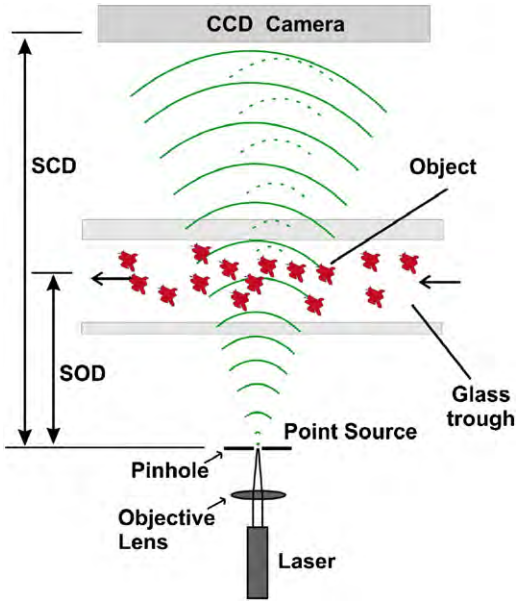

Fig. 1. Schematic of DIHM. Light from a laser is focused onto a pinhole. The emerging spherical wave illuminates the object which in this illustration is a glass trough for the flow of particles. At the CCD camera the scattered waves (dotted arcs) interfere with the reference waves (solid arcs) to produce a hologram. By varying the SOD (source to object distance) and the SCD (source to camera distance) different levels of magnification can be obtained.

gram pairs, pixel by pixel, to generate new holograms, i.e. (h_1-h_2), (h_3-h_4), etc. (iii) The resultant difference pictures are summed (a few hundred holograms could be combined) into a single file, which now contains all holograms (albeit with alternate sign), yet has the same size as any single original hologram. Subtracting alternate holograms ensures that the dynamic range is not exceeded and that only the object-related-information (moving algae, latex beads or red blood cells, as examples) is retained.

Holography is a two-step process: first, a hologram must be recorded, and second, reconstruction must yield an "image" of the object, i.e. the intensity of the wavefront at the object. The role of reconstruction is to obtain the three-dimensional structure of the object from the two-dimensional hologram on the screen, or, in physical terms, to reconstruct the wave front at the object. This can be achieved via a Kirchhoff–Helmholtz transform [8]

$$K(\mathbf{r}) = \int_{\text{screen}} d^2\xi \tilde{I}(\xi) \exp[\mathrm{i}kr \cdot \xi/|\xi|] \tag{1}$$

in which the integration extends over the two-dimensional surface of the screen with coordinates $\xi = (X,Y,L)$ where L is the distance from the source (pinhole) to the center of the screen (CCD chip); and $\tilde{I}(\xi)$ is the contrast image (hologram) on the screen obtained by subtracting the images with and without the object present. The function $K(\mathbf{r})$ is significantly structured and different from zero only in the space region occupied by the object. By reconstructing the wave front $K(\mathbf{r})$ on a number of planes at various distances from the source in the vicinity of the object, a three-dimensional image can be built up from a single two-dimensional hologram. $K(\mathbf{r})$ is a complex function and one usually plots the intensity $|K(\mathbf{r})|^2$ to represent the object, although phase images are also available. For the numerical implementation of the transform a fast algorithm has been developed that evaluates $K(\mathbf{r})$ without any approximations [9]. It employs a coordinate transformation to remove the nonlinearity in the exponential that transform the integral into a convolution that is solved by three consecutive 2-D fast Fourier transforms. This allows a choice of the size of the reconstructed image so that one can magnify different parts of the object at will.

In holography, the term "reconstruction" is used to obtain the function $K(\mathbf{r})$ from the hologram. The plot of $|K(\mathbf{r})|^2$ on a two-dimensional plane, which we will call a 2-D holographic reconstruction, is equivalent to one in-focus image taken in a conventional compound microscope. In DIHM one can generate a stack of 2-D holographic reconstructions from a single hologram. Combining such a stack will result in a three-dimensional image of the object; this latter step is usually referred to as 3-D reconstruction or 3-D rendering.

3. Experimental results

In a first set of experiments we attached a sphere of diameter 150 μm to the top of a tank 1.5 mm wide filled with water seeded with 5 μm latex beads to a depth of 300 μm. Using blotting paper as a suction pump the water is made to flow from left to right. Once steady state is achieved we took a series of 90 holograms at time intervals of 0.17 s, and combined them into a single difference hologram, panel A in Fig. 2, from which we made 60 holographic reconstructions one of which is shown in panel B. The distance between successive positions of a given bead along its trajectory is proportional to the local fluid velocity. The velocity field is plotted in panel C. We have color-coded the height from the bottom of the tank (blue) to the top (red). The speed far from the sphere on the left and right is 50 μm/s. Needless to say this velocity field agrees perfectly with Navier–Stokes' solution (solid blue lines in panel D).

Next we have put two large spheres into the trough either behind each other along the dominant fluid flow or perpendicular to it. As the flow indicator we have used red bovine blood cells in a 310 mOsm NaCl solution, their average size is about 10 μm. One hundred holograms were taken at 10 frames per second and combined into a difference hologram for each experiment. Resulting flow patterns are shown in Figs. 3 and 4. Again we have used Stokes' equation to calculate these flow patterns and found perfect agreement. Note that in Fig. 3 (panels B and D) some trajectories are partially obscured where they are behind the spheres. The full symmetry of the flow observed panel A of Fig. 3, is not presented in panels C and D of the same figure due to turbulences between the spheres.

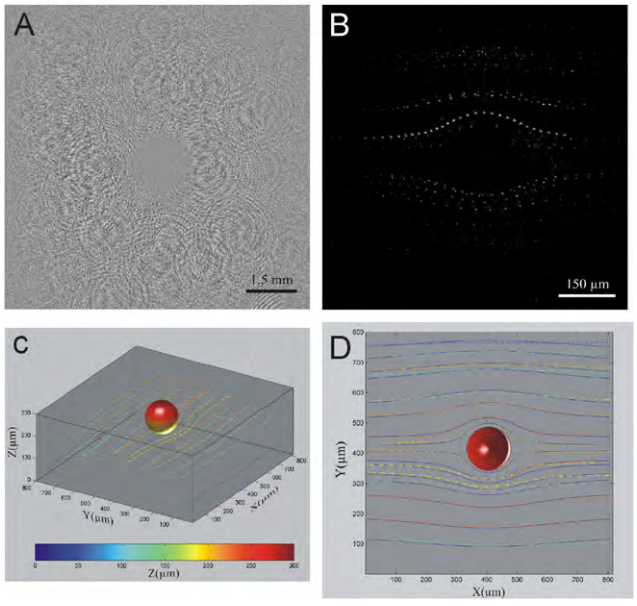

Fig. 2. Stokes' flow around a fixed sphere. 90 holograms were taken at intervals of 0.17 s to generate a difference hologram, panel A. Panel B shows one of 60 reconstructions made to render the field velocity shown in panel C. In panel D the solid blue lines represent the solution to the Navier–Stokes equation for our experiment and the arrows correspond to the measured velocity field. We have used a green laser illuminating a 1 μm pinhole. Pinhole to sample distance 1 mm and numerical aperture of 0.25.

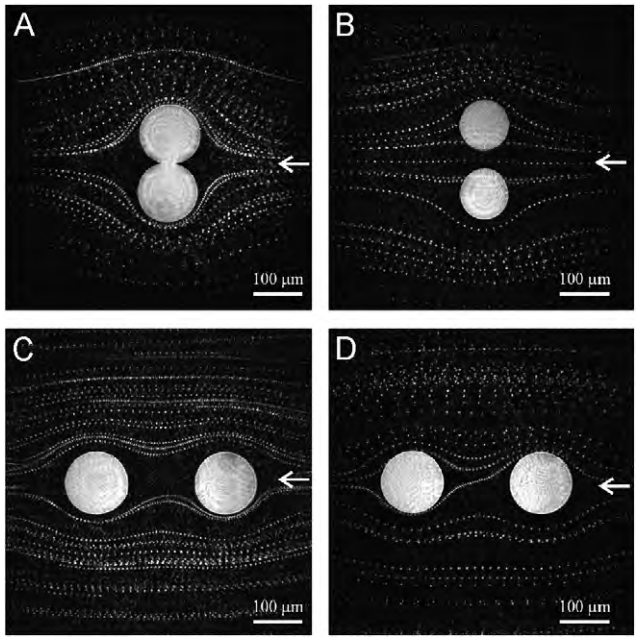

Fig. 3. Bovine red blood cells flow around two spheres in different geometries fixed to the bottom of the tank. Flow is in direction of the arrows. Reconstructions from a difference hologram composed of 100 holograms taken at 10 frames per second, are on the equatorial plane parallel to the bottom of the tank. A green laser was used to illuminate a 1 μm pinhole. Pinhole to sample distance 1 mm and numerical aperture of 0.25.

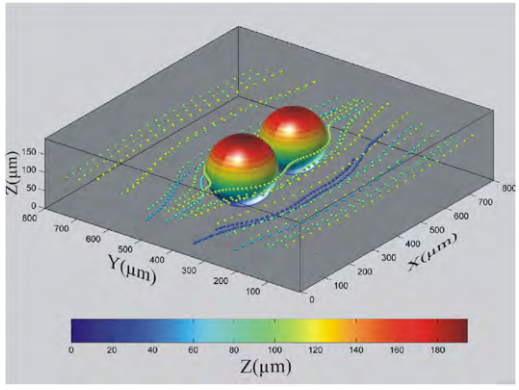

Fig. 4. 3-D rendering of flow of bovine red blood cells. 50 reconstructions on different planes 3.8 μm apart, similar to the ones shown in Fig. 3 panel A. The 3-D rendering was done with MATLAB®. The blood cells are represented by enlarged spheres for easier viewing.

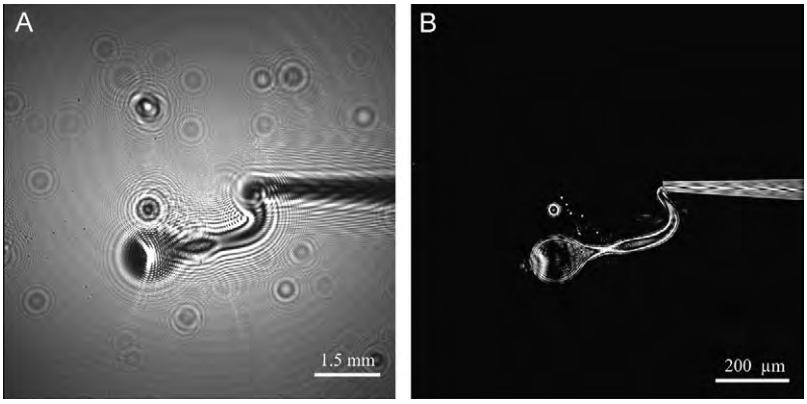

Fig. 5. Injection of oil (Triton® X-100) into distilled water. Panel A shows the 30th hologram of a series of 60 taken at 5 frames per second with a green laser illuminating a 1 μm pinhole; pinhole to sample distance 2 mm and numerical aperture of 0.22. Reconstruction of 1 of the 60 holograms at its best focal plane.

To obtain a 3-D rendering of the flow pattern we have performed 50 holographic reconstructions at different planes from a difference hologram; the corresponding reconstruction for the equatorial plane is shown in panel B of Fig. 3. Locating the maxima intensity of each position of all cells within this stack of data we have used these positions in a 3-D rendering tool developed in MATLAB® in which we have represented the cells by enlarged spheres for easier viewing. We have again color-coded the height from the bottom of the tank (blue) to the top (red). A film showing the flow pattern from all sides (including close-ups) is presented in Fig. 4.

As another application of DIHM in fluid dynamics we have studied the injection of oil (Triton® X-100) into water through a capillary syringe with an opening of 10 μm. To follow the dispersion of the oil we have taken 60 holograms at 10 frames per second. As an example we show in Fig. 5 panel A the hologram number 30 taken 6 s after the beginning of the injection.

Next we have reconstructed these holograms in the best focal planes and assembled them into a movie to dynamic studies (on the frames is shown in Fig. 5 panel B). As pressure is manually applied to the syringe oil spouts out and very quickly pinches off a few large and many tiny bubbles as small as 6 μm that disperse into the water. As the pressure on the syringe is released the oil retracts back into the capillary due to surface tension. This information can be extracted from the movie available for the readers upon request.

We emphasize the efficiency in data collection in our procedure. Removal of background effects and construction of summed holograms are easily accomplished so that high-resolution tracking of many particles in 4-D from just a single hologram data set can be performed. Since resolution on the order of the wavelength of light is routinely achieved with DIHM, tracking of organisms as small as bacteria is possible, as would the motion of plankton in water or, at lower resolution, the aerial trajectories of flying insects. Outside of biology, applications of 4-D DIHM are possible in particle velocimetry, i.e. tracking of the motion of particles in a liquid or gas flows, visualization of structures in convective or turbulent flow and in colloidal suspensions, remote sensing and environmental monitoring, investigation of bacterial attachment to surfaces and biofilm formation, and many more.

Acknowledgments

This work was supported by NSERC, the Natural Sciences and Engineering Council of Canada and by the Office of Naval Research.

References

[1] J.P. Brody, P. Yager, R.E. Goldstein, R.H. Austin, Biotechnology at low Reynolds numbers, Biophys. J. 71 (1996) 3430–3441.
[2] A. Hatch, A.E. Kamholz, K.R. Hawkins, M.S. Munson, E.A. Schilling, B.H. Weigl, P. Yager, A rapid diffusion immunoassay in a T-Sensor, Nat. Biotechnol. 19 (2001) 461–465.
[3] J. Yang, Y. Huang, X.B. Wang, F.F. Becker, P.R.C. Gascoyne, Cell separation on microfabricated electrodes using dielectrophoretic/gravitational field flow fractionation, Anal. Chem. 71 (1999) 911–918.
[4] C.D. Meinhart, S.T. Wereley, J.G. Santiago, Micron-resolution velocimetry techniques, in: E.D.R.J. Adrian, et al. (Eds.), Developments in Laser Techniques and Applications to Fluid Mechanics, Springer, Berlin—Germany, 1998.
[5] C.D. Meinhart, S.T. Wereley, J.G. Santiago, PIV measurements of a microchannel flow, Exp. Fluids 27 (1999) 414–419.
[6] J.G. Santiago, S.T. Wereley, C.D. Meinhart, D.J. Beebe, R.J. Adrian, A particle image velocimetry system for microfluidics, Exp. Fluids 25 (1998) 316–319.

[7] W. Xu, M.H. Jericho, I.A. Meinertzhagen, H.J. Kreuzer, Tracking particles in 4-D with in-line holographic microscopy, Opt. Lett. 28 (2003) 164–166.
[8] H.J. Kreuzer, K. Nakamura, A. Wierzbicki, H.-W. Fink, H. Schmid, Theory of the point source electron microscope, Ultramicroscopy 45 (1992) 381–403.
[9] H.J. Kreuzer, R.A. Pawlitzek, LEEPS Version 1.2, A Software Package for the Simulation and Reconstruction of Low Energy Electron Point Source Images and Other Holograms, Helix Science Applications, Halifax, NS, Canada, 1993–1998.
[10] W. Xu, M.H. Jericho, I.A. Meinertzhagen, H.J. Kreuzer, Digital in-line holography of microspheres, Appl. Opt. 41 (2002) 5367–5375.
[11] J. Garcia-Sucerquia, W. Xu, S.K. Jericho, P. Klages, M.H. Jericho, H.J. Kreuzer, Digital in-line holography microscopy, Appl. Opt. 45 (2006) 836–850.